Proceedings of IDETC/CIE 2009
the ASME 2009 International Design Engineering Technical Conferences & Computers and Information in Engineering Conference
August 30 - September 2, 2009, San Diego, California, USA

ASME2009-86847

DESIGN OF A TUNABLE STIFFNESS COMPOSITE LEG FOR DYNAMIC LOCOMOTION

Kevin C. Galloway *
Mechanical Engineering
and Applied Mechanics
University of Pennsylvania
Philadelphia, PA 19104
Email: kcg@seas.upenn.edu

Jonathan E. Clark
Mechanical Engineering
Florida A&M - Florida State University
Tallahassee, FL 32310

Daniel E. Koditschek
Electrical and Systems Engineering
University of Pennsylvania
Philadelphia, PA 19104

ABSTRACT

Passively compliant legs have been instrumental in the development of dynamically running legged robots. Having properly tuned leg springs is essential for stable, robust and energetically efficient running at high speeds. Recent simulation studies indicate that having variable stiffness legs, as animals do, can significantly improve the speed and stability of these robots in changing environmental conditions. However, to date, the mechanical complexities of designing usefully robust tunable passive compliance into legs has precluded their implementation on practical running robots. This paper describes a new design of a "structurally controlled variable stiffness" leg for a hexapedal running robot. This new leg improves on previous designs' performance and enables runtime modification of leg stiffness in a small, lightweight, and rugged package. Modeling and leg test experiments are presented that characterize the improvement in stiffness range, energy storage, and dynamic coupling properties of these legs. We conclude that this variable stiffness leg design is now ready for implementation and testing on a dynamical running robot.

I. INTRODUCTION

Animals, unlike most current robotic systems, are able to adjust the physical properties of their limbs as well as their control parameters to help them adapt to changing conditions in their environment [1] [2]. One of the challenges in the field of robotic legged locomotion is to develop active, programmable mechanisms to endow robotic structures with the kind of adaptability and robustness found in biological systems. Recent work in robotic leg locomotion has attempted to close this performance gap by incorporating tunable mechanical leg stiffness [3] [4]. The hypothesis behind this approach is that tuned resonant running leads to energy efficient and stable locomotion. Matching the leg stiffness to the leg swing frequency can minimize the amount of motor work that must be inserted during each stance phase. Recent work by [5] suggests that tunable leg stiffness can be used to improve robot speed and stability. These simulation studies demonstrated that tuning leg stiffness alone in response to changes in robot mass yielded better results than those obtained by optimizing the controller alone. This result is particularly significant as it was conducted on a model based on Edubot [6] (see Fig.1), a RHex-like hexapedal robot [7] [8], which serves as the target platform for our leg design.

Further motivation for designing legs that can individually adjust their stiffness comes from studies of leg specialization in multi-legged runners. Functional specialization in the front, middle, and rear legs of hexapedal runners can contribute to their stability [9], and running quadrupeds may respond faster to perturbations in ground height if leg stiffness is increased [10]. Together the evidence suggests that run-time alteration of the passive compliance of individual pairs of legs may allow a robot to

*Address all correspondence to this author.

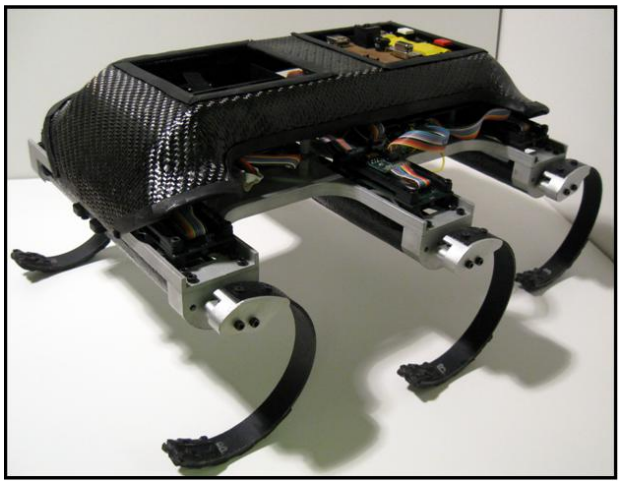

Figure 1. EDUBOT, A HEXAPEDAL DYNAMIC LEGGED LOCOMOTION PLATFORM [6].

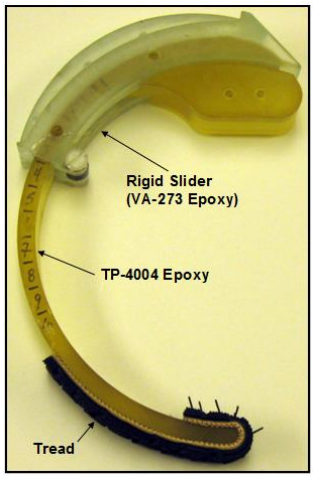

Figure 2. PREVIOUS DESIGN: STRUCTURAL CONTROLLED STIFFNESS LEG USING A RIGID SLIDER [4].

more successfully adapt to changes in the running environment.

The first effort to incorporate the passive mechanical compliance of a robot's legs machine yielded the springy C-legs we continue to use today [11]. There have been several methods proposed for mechanically adjusting leg stiffness, each with its advantages and disadvantages. In one design for a bipedal system, the Biped with Mechanically Adjusted Series Compliance (BiMASC) uses an antagonistic set-up of two non-linear fiberglass springs to store and return energy [12]. A complex system of cables and two motors adjust the set point and pretension on the fiberglass springs. Although the device demonstrated variable stiffness it proved inefficient at storing and returning energy during hopping. This was attributed to the fact that in an antagonistic spring arrangement only one spring actually compresses to store energy while the other relaxes to transfer energy into the compressing spring [12]. Furthermore, the internal forces generated by antagonistic spring arrangements increases the frictional losses of the system [12]. There have been other attempts to achieve tunable stiffness using antagonistic pneumatic actuators such as McKibben actuators and pleated pneumatic artificial muscle [13] [14]. Although stiffness control has been achieved through pneumatic actuation, the power requirements for pneumatics make it difficult to implement on any autonomous dynamic legged locomotion system.

Another approach, perhaps better suited for implementation on small robots, is the method of structural controlled stiffness where a mechanical change in the device alters the stiffness of a spring element. For example, in [15] a passive spring element is constructed from several layers of flexible sheets. The mechanical impedance of the passive element is adjusted by controlling the connectivity of the layers through an external stimulus such as a vacuum. In another example, the mechanical impedance of robot finger joints is adjusted by changing the effective length of a leaf spring [16]. Hollander et al [17] also propose a tunable helical spring concept in which stiffness is adjusted by controlling the number of active coils.

In our previous work [4], a tunable leg design was presented whereby leg stiffness was adjusted by sliding an element along the length of Edubot's "C-shaped" compliant legs (see Figure2). The portion of the leg covered by the element was assumed to be rigid, while the remaining exposed portion was considered the compliant. While it was demonstrated that the overall stiffness could be varied by as much as 90% there were some undesirable features coupled in the design including: altered tip deflection trajectory, shifted mass moment of inertia, and increased probabilitiy of inelastic collisions.

Maintaining consistent tip trajectory for the continuous range of stiffness settings is an important feature to consider in a tunable leg. In our previous design each stiffness setting altered the deformation tendency of the leg spring. In other words, the deflection path of the leg spring would respond differently to applied loads depending on the stiffness setting. Such configurations make it difficult to determine whether a tunable leg performed better or worse due to the change in stiffness or to the altered deformation behavior.

Increasing the stiffness of the leg spring with a rigid slider introduces another undesirable feature by shifting the center of mass. Making a slider rigid requires a more massive structure to resist deformation during the stance phase. Adjusting the rigid slider position to increase leg stiffness causes the leg moment of inertia to shift away from the axis of rotation. This can significantly increase the loads on the motor due to leg acceleration changes during each stride.

One of the novel features of the original passive compliant

C-shaped legs [11] is that they enable the robot to navigate rough terrain by allowing compliant ground contact anywhere along the length of the leg. A leg design with a rigid slider effectively limits the leg length that is capable absorbing impacts. This is important to consider as legs are generally stiffer at higher speeds where the potential for damage from collisions is greatest.

In this paper we present a variable stiffness leg design that overcomes the drawbacks of the rigid slider configuration (our previous design), improves the efficiency of the leg, and incorporates an actuation system to enable autonmous stiffness adjustment. The remainder of the paper describes these advances in the following manner. In section II, we describe the design of a new composite tunable leg and discuss its advantages over previous designs. In particular we describe the compliant slider design and material property considerations. Section III offers a combined Pseudo-Rigid Body (PRB) modeling and finite element analysis approach for designing tunable legs (or any tunable element) to achieve desired stiffness ranges, and section IV describes the bench top experimental studies used to characterize the behavior of the new composite legs. Section V summarizes the results of the paper and describes future work.

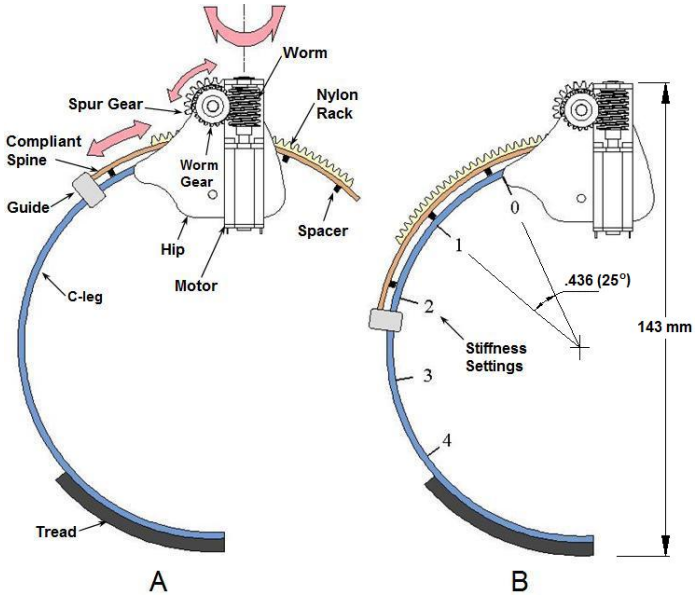

Figure 3. PROPOSED NEW DESIGN: SIDE VIEW OF TUNABLE STIFFNESS COMPOSITE LEG DESIGN. A) ILLUSTRATES THE ROTATION DIRECTIONS OF GEARS B) ILLUSTRATES THE SPINE AJUSTED TO A HIGHER STIFFNESS SETTING.

II. STRUCTURAL CONTROLLED STIFFNESS LEG WITH COMPLIANT SPINE

The shortcomings of previous variable stiffness leg designs have motivated the design of a new structurally controlled stiffness robot leg. Our goal is to provide a small, light, and robust limb that can be employed on a robot to empirically test the proposed advantages of variable compliance limbs in running. In particular, we aim to ensure that the effect of changing stiffness is not confounded with other factors, such as leg length, damping, or deflection path. To achieve this goal this section describes a 'C-Shaped' leg with a novel compliant spine. We describe the design of the mechanism to slide the spine as well as the material selection and property choices which led to the selection of the particular composite structure chosen– S2-6781 pre-preg fiberglass (Applied Vehicle Technologies, Inc., Indianapolis, IN) (see Figure 3).

Compliant Spine Mechanism

Our research suggests that replacing the rigid slider with a compliant spine offers a significant variability in effective stiffness while still overcoming the drawbacks found in a our previous work. In the new design, the leg is anchored to an aluminum hip structure which also supports the drive mechanism. A thin, flexible rack is anchored to the back of the compliant spine, and controls the spine position without significantly altering the spine stiffness. The position of the spine can be adjusted by activating a small, geared DC motor mounted to the hip, which simultaneously drives a nylon worm and spur gear (see Figure 4). A small aluminum guide is attached at one end of the spine and wraps around the C-leg. The guide holds the spine against the C-leg, and acts as a mechanical stop when the spine is actuated to softest stiffness setting. The spacing between the C-leg and the compliant spine is approximately 1.5 mm. It is important to maintain this spacing so that the two compliant elements deform together under load. To enforce this condition, small spacers were attached to the inside surface of the compliant space.

During operation, the motor can rotate clockwise or counterclockwise to move the slider through the continuous spectrum of leg stiffnesses. When the slider reaches a target stiffness setting, the motor shuts off, and the worm provides sufficient resistance to rotation in either direction; thus acting as a natural self-locking mechanism. Hence no power is required to maintain a desired leg stiffness during locomotion. This also results in a robust and efficient spring as there are no moving parts for a given stiffness setting. In its final configuration, the tunable C-leg has a 114 mm inner diameter and weighs less than 85 grams.

Material Selection

As with any passive compliant spring mechanism, the material property of the spring element and shape dictate its ability to store and return energy. Important material properties to consider for any elastic element include its density, Young's modulus, yield strength, fatigue life, energy storage density, and manufacturability.

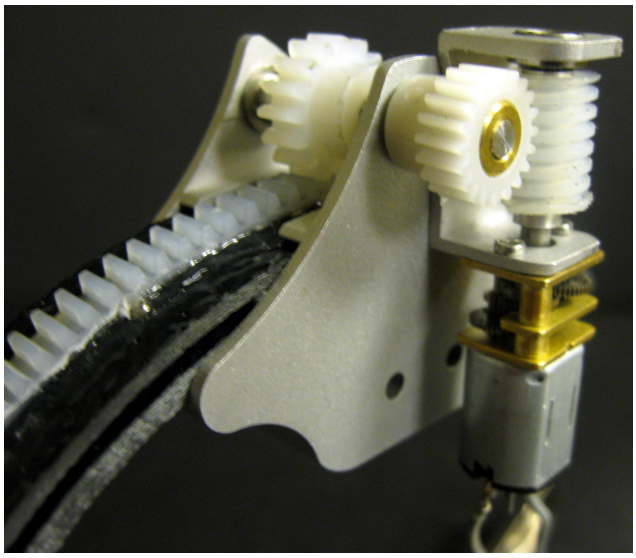

Figure 4. ACTIVE COMPONENT OF NEW DESIGN: IMAGE OF THE PROTOTYPED VARIABLE STIFFNESS LEG.

Material	ρ (g/cc)	E (Gpa)	S (Mpa)	(S/E) x10^3	U x 10^3 (J/kg)	$ (USD) per leg
Aluminum 7075-T6	2.81	71.7	500	7.0	1.24	1
Fiberglass (S2-6781)	2.25	22	400+	18.2	3.23	3
Nitinol	6.50	1	1000	1333	6.8*	30+
Steel (4140 Q&T@400)	7.75	207	238	1.1	0.04	2.5
TP-4004 (Epoxy)	1.17	0.80	34	42.5	1.24	6

*Duerig et al., "Engineering Aspects of Shape Memory Alloys," 1990.

Figure 5. COMPARISON OF MATERIAL PROPERTIES.

Some of the materials we have used to prototype legs include plastic, nitinol, aluminum and glass fiber composites. These materials and some of their properties are listed in Figure 5 where ρ is the density, E is the Young's Modulus, S is the ultimate yield strength, S/E is the yield strength to Young's modulus ratio, and U is the specific strain energy of the material which is expressed as

$$U = \frac{S^2}{\rho E} \tag{1}$$

It can be observed that the materials with the best specific strain energy capacity are those with a large yield strength and a low density and Young's modulus [18].

In our earlier design, shape deposition manufacturing (SDM) [19] was used to manufacture legs from an epoxy (TP-4004 Innovative Polymers, Inc., Saint Johns, MI). Epoxies come

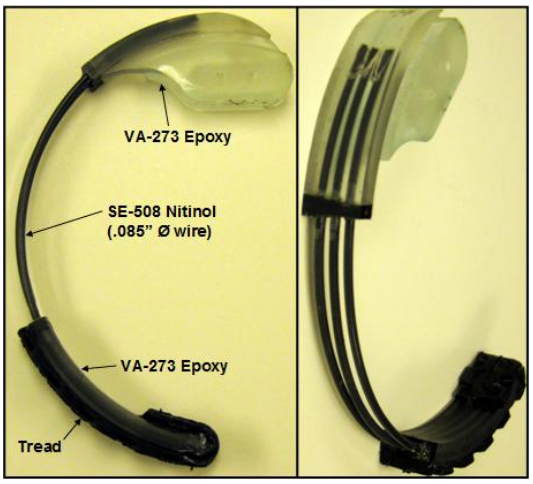

Figure 6. OLDER DESIGN ALTERNATIVE: C-LEG WITH A NITINOL SPRING ELEMENT.

in a wide range of Young's modulus and yield strength values and through SDM, one can manufacture consistent parts with arbitrary geometries using wax molds. However, the fatigue life of epoxy is generally not optimal for the application of dynamic locomotion where legs are cyclically loaded under various and often unpredictable conditions and, in fact, many of these legs cracked during extended testing.

Nitinol is another material that was considered mainly for its high energy density and yield strength. As an elastic element, nitinol offers attractive properties including the ability to recover from bending strains as large as 10% without plasticly deforming (note: spring steel can manage about 0.2% strain before plastic deformation), and a low Young's modulus. However, nitinol has less desirable properties, including a high raw material cost, limited available stock geometries, hysteresis, and difficulty to form various geometries with tight tolerances. For exmaple, in order to achieve a desired curvature, nitinol must be clamped to a custom mold and baked at temperatures of 530°C. Several legs were fabricated using this technique and SDM was used to embed them into a plastic hip structure (see Figure 6); however, achieving consistant radius and stiffness values from leg to leg proved very difficult.

Composite laminate, specifically S2-6781 pre-preg fiberglass, was eventually selected as the material of choice for several reasons including its relatively low density and Young's modulus, high yield strength, comparatively high specific strain energy capacity and low material cost. In addition to these properties, composite laminates expand the available design space by offering the ability to change the Young's modulus value. The isotropic nature of the other materials considered (i.e. metal and plastic) often leads to situations where a desired spring element geometry such as the moment of inertia, does not have the yield

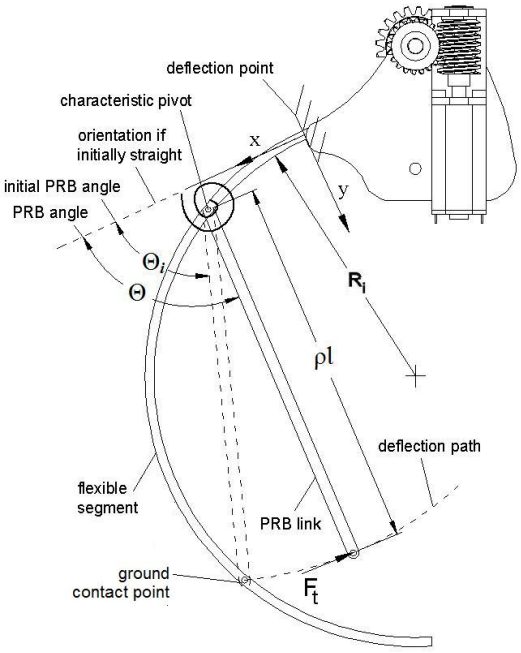

Figure 7. PSEUDO-RIGID-BODY MODEL APPLIED TO THE C-LEG. ADAPTED FROM [21] and [4]

strength to withstand the demands of the intended environment which include stresses caused by changing payloads, speeds, irregular landings and collisions. Many composites, including the fiberglass composite chosen, are anisotropic and thus have properties that change depending on the orientation along which the property is measured [20]. By laying the plies in certain orientations during the manufacturing process, one can change the Young's modulus of a composite material by a factor of two or more. Thus, compared to isotropic materials, the stiffness of a spring element constructed from an anisotropic material is less dependent on the spring geometry.

III. LEG STIFFNESS MODEL

To estimate the stiffness range of the compliant C-leg with a compliant spine, we employ the pseudo-rigid-body (PRB) model [21] as we did in [4] from which we have adapted the following description of the method. The PRB is an appropriate choice of a model as it accurately captures the large non-linear deflections of the C-leg under an applied load with a very small investment of time. In the PRB model, flexible members are represented as rigid links connected via hinge or pin joints with torsional springs. In this model, the initial curvature and leg length are related through the non-dimensionalized parameter

$$k_o = \frac{l}{R_i} \tag{2}$$

where l is the leg arc length measured along the centroidal axis of the leg from the point of deflection to the point of the applied loading, and R_i is the initial radius of the curved beam. Figure 7 details the components of the PRB model where the characteristic radius factor, ρ, is used to determine the location of the the characteristic pivot and the length of the pseudo-rigid-body link. The PRB angle, Θ, specifies the angle of the PRB link while, Θ_i, defines the initial angle of the PRB link. Detailed explanations of the PRB model can be found in [22]; however, for this work we are primarily interested in the magnitude of the torsional spring constant, K_t, which is given by

$$K_t = \rho K_\Theta \frac{EI}{l} \tag{3}$$

where K_Θ is the stiffness coefficient, E is the Young's modulus, and I is the moment of inertia in the sagittal plane. For a given k_o value, ρ and K_Θ can be averaged for a range of loading conditions, but more conveniently, approximations have been captured in a simple look-up table in [21]. Therefore, E, I, R_i, and l are all that is needed to approximate K_t. Currently the PRB model can only be applied to approximate the stiffness of the C-leg at its softest and stiffest settings.

When the tunable leg is at the stiffest setting, we have found that the effective moment of inertia is best expressed as

$$I_{effective} = I_{leg} + I_{spine} \tag{4}$$

where I_{leg} is equal to $b_{leg}h_{leg}^3/12$ and I_{spine} is expressed as

$$I_{spine} = \frac{E_{spine}b_{spine}h_{spine}^3}{12E_{leg}} \tag{5}$$

This formulation is an adaption of the one presented in [15]. The ratio of E_{spine} to E_{leg} is a common expression used to account for situations in which members subject to bending are made of more than one material. With composite materials it is easy to fabricate the leg and spine for two very different Young's moduli.

Since the PRB model assumes a uniform cross-section, the model cannot be used to estimate the leg stiffness range and tip trajectory at intermediate stiffness settings. The finite element method can be used to produce the needed information; however, this requires a larger investment of time. To expedite the

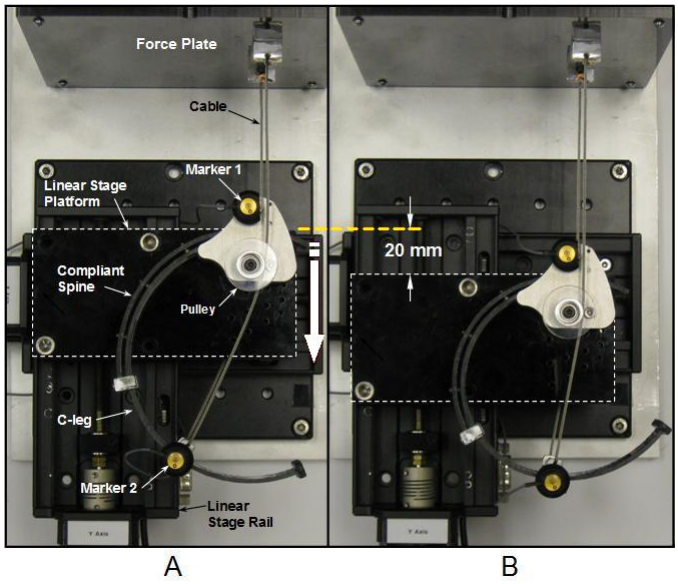

Figure 8. TOP VIEW OF EXPERIMENTAL SET-UP. A) LINEAR STAGE IS IN THE HOME POSITION AND LEG IS UNDEFLECTED. B) PLATFORM HAS BEEN MOVED A DISTANCE ,d, AND LEG IS DEFLECTED.

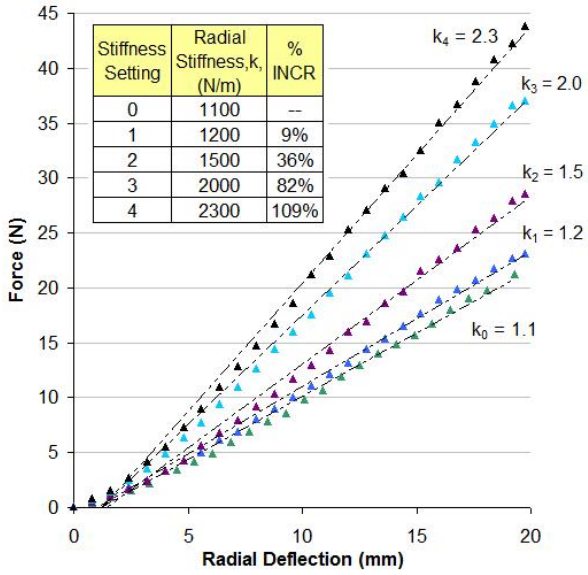

Figure 9. SPRING FORCE RESPONSE AT FOUR DIFFERENT LEG STIFFNESS SETTINGS EACH WITH A CURVE FIT (DOTTED LINE) APPLIED TO LOADING PHASE.

design process, we have determined that a stiffness setting near the angular position of 50° (see Figure 3B) leads to the greatest tip trajectory deviation. Therefore if one can design the tip trajectory at this setting to approximately match the behavior at the stiffness extremes, then the intermediate settings should also closely approximate the same behavior. Preliminary and ongoing work is underway to modify the PRB model to capture the compliance of an initially curved stepped cantilever beam as two or more torsional springs in series.

IV. EXPERIMENTAL LEG CHARACTERIZATION

To observe the leg deflection behavior and to validate the PRB model, an experimental apparatus was constructed to measure an applied load and to record the resulting deflection path. In the present experiment a Micos linear stage and an AMTI HE6x6 force plate were rigidly connected to an aluminum base plate. The linear stage has a resolution of one micrometer and is capable of traveling 80 mm at rates as high as 14 mm/s. The AMTI HE6x6 is a six axis force plate capable of measuring loads as large as 16 pounds at 200hz with 12-bit resolution. The C-leg's aluminum hip was anchored to the linear stage platform and the C-leg was cantilevered out from the platform. An aluminum clamp was affixed to the leg at the position indicated by Marker 2 in Figure 8A. One end of a flexible steel cable was anchored to the force plate while the other was connected to the leg clamp. A pulley was anchored to the hip to provide a rolling contact point and to make the cable normal to the the force plate's surface. The linear stage was commanded to translate (see Figure 8B) the hip a distance of 20 mm at 10 mm/s in the y-direction (given by large downward pointing white arrow on the right side of Figure 8A). The force plate collected the reaction forces at the loading point (Marker 2) at a sampling rate of 200 Hz. An Optotrak 3020 motion capture system was used to capture the position of Markers 1 and 2 also at a sampling rate of 200 Hz. This was repeated for each of the leg stiffness settings 0-4 by shifting the compliant spine (see Figure 3B) along the length of the C-leg. The 6-ply fiberglass C-leg and spine were constructed with an alternating 50/50 blend ratio where 50% of the plies where angled at 45° while the other half were angled at 0°. The leg inner diameter is 114 mm with a thickness of 2.25 mm and a width of 18 mm. We estimate the Young's modulus value to be 9.65 GPa.

Stiffness Results

In Figure 9 the experimental results of the load measured against the deflection in the radial direction demonstrate that the stiffness increases monotonically. The stiffness, which is indicated as a slope value, k, next to each curve, doubled between the two stiffness extremes. This was expected as the only difference between the two extremes was a doubling of the moment of inertia. Its also worth noting that the stiffness increase from leg stiffness setting (LSS) 0 and LSS1 is approximately 9% for this configuration. In future models, LSS1 could be the home position to allow the leg to reach higher stiffness settings faster without significantly limiting the stiffness range.

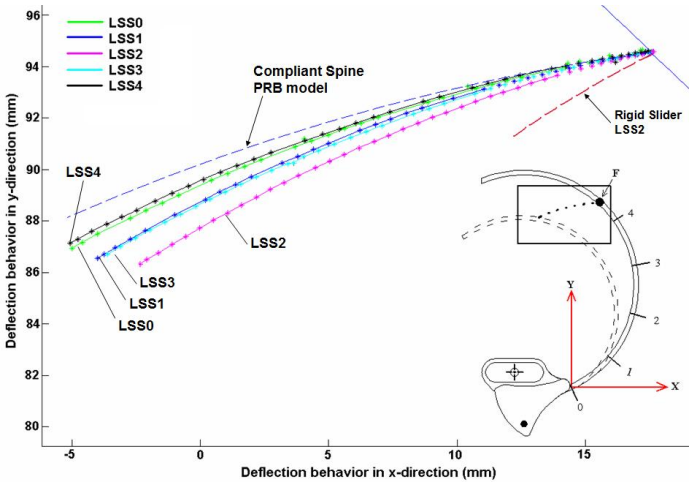

Figure 10. DEFLECTION PATH OF LEG FOR VARIOUS STIFFNESS SETTINGS.

Deflection Orientation Results

In Figure 10 the actual xy-deflection of the leg under load is presented. The bottom right image in Figure 10 provides a bearing for the location and orientation of the xy-axis while the rectangle reflects the results window. For the range of the stiffness settings the deflection paths showed low variability. In particular, the deflection path of the two extreme stiffnesses (i.e. LSS0 and LSS4) were almost identical and varied by no more than 0.5 mm from each other. At maximum deflection, these results were also within 1 mm of the deflection path predicted by the compliant spine PRB model, which for a total deflection of 20 mm in the y-direction, represents about a 5% estimation error. As expected, the deflection path at LSS2 showed the most deviation. At maximum deflection, the y-component deviation was approximately 2 mm which represents roughly a 10% difference from the compliant spine PRB curve. For comparison purposes, the same tangential force that produced the deflection path for LSS2 was applied to a rigid slider PRB model also at LSS2. The rigid slider tuning method clearly produces very different spring behavior (see curve labled 'Rigid Slider LSS2'). The stiffness is much larger given by the short deflection path, and the characteristic radius is much shorter creating a steep deflection path. It should be noted that achieving consistent deflection behavior for all stiffnesses while achieving a large deflection range are two competing objectives. If the compliant spine is too soft then the deflection path will be consistent; however, the stiffness range will be very small. Similarly, if the compliant spine is too stiff, the deflection path and stiffness range will begin to reflect the rigid slider model. Therefore, while deviation in deflection behavior is expected through proper material selection and geometries this can be minimized while still achieving a considerable stiffness range.

Conclusions and Future Work

Tunable legs have the potential to allow autonomous robots to locomote with improved efficiency, stability, and animal-like agility [1]. As part of our ongoing work to study tunable legs for dynamic locomotion, we have developed a robust, self-locking, structurally controlled, tunable stiffness leg for implementation on a dynamic hexapedal robot. We have shown that with a proper selection of materials and geometries, the proposed tunable leg can achieve a 100% or more change in stiffness without a significant change in deflection behavior. Several materials have been considered; however, we have found that composite materials offer the best combination of energy storage capacity, high yeild strength, ease of manufacturing, and Young's modulus control.

In the near future, we will explore through experimentation on Edubot the benefits and costs of mechanically tuning leg compliance. It is our intention that these new tunable legs will be used on our robotic platform to experimentally validate simulation results and hypotheses about the effect of variable stiffness legs on the stability and efficiency of legged locomotion.

ACKNOWLEDGMENT

We would like to thank Dr. Larry L. Howell and Christopher E. Thorne for their input and support. This work was also partially supported by the NSF FIBR grant #0425878.

REFERENCES

[1] Alexander, R. M., 1990. "Three uses for springs in legged locomotion". *International Journal of Robotics Research,* **9**(2), pp. 53–61.

[2] Ferris, D., Louie, M., and Farley, C., 1998. "Running in the real world: Adjusting leg stiffness for different surfaces". In Proceedings of the Royal Society London, Vol. 265, pp. 989–993.

[3] Hurst, W., C. J. E., and Rizzi, A., A., 2004. "An actuator with physically variable stiffness for highly dynamic legged locomotion". In Proceedings - IEEE International Conference on Robotics and Automation, pp. 4662–4667.

[4] Galloway, K., Clark, J., and Koditschek, D., 2007. "Design of a multi-directional variable stiffness leg for dynamic runnings". In ASME Int. Mech. Eng. Congress and Exposition.

[5] Yun Jun, J., and Clark, J., 2009. "Dynamic stability of variable stiffness running". In International Conference on Robotics and Automation, IEEE.

[6] Weingarten, J., Koditschek, D., Komsuoglu, H., and Massey, C., 2007. "Robotics as the delivery vehicle: A contexualized, social, self paced, engineering education for life-long learners". In RSS Workshop on Research in Robots for Education.

[7] Altendorfer, R., Moore, N., Komsuoglu, H., Buehler, M., Brown H. B, J., McMordie, D., Saranli, U., Full, R., and

Koditschek, D. E., 2001. "Rhex: A biologically inspired hexapod runner". *Autonomous Robots,* **11**(3), pp. 207–213.
[8] Saranli, U., Buehler, M., and Koditschek, D. E., 2001. "Rhex: A simple and highly mobile hexapod robot". *International Journal of Robotics Research,* **20**(7), pp. 616–631.
[9] Clark, J. E., 2004. "Design, simulation, and stability of a hexapedal running robot". PhD thesis, Stanford University.
[10] Meek, S., Kim, J., and Anderson, M., 2008. "Stability of a trotting quaduped robot with passive, underactuated legs". In IEEE International Conference on Robotics and Automation, pp. 347–351.
[11] Moore, E. Z., Campbell, D., Grimminger, F., and Buehler, M., 2002. "Reliable stair climbing in the simple hexapod 'rhex"'. In Proceedings - IEEE International Conference on Robotics and Automation, Vol. 3, pp. 2222–2227.
[12] Hurst, J., 2008. "The role and implementation of compliance in legged locomotion". PhD thesis, Carnegie Mellon University.
[13] Verrelst, B., Van Ham, R., Vanderborght, B., Daerden, F., Lefeber, D., and Vermeulen, J., 2005. "The pneumatic biped lucy actuated with pleated pneumatic artificial muscles". *Autonomous Robots,* **18**, pp. 201–213.
[14] Takuma, T., Hayashi, S., and Hosoda, K., 2008. "3d bipedal robot with tunable leg compliance mechanism for multi-modal locomotion". In IEEE/RSJ International Conference on Intelligent Robots and Systems.
[15] Kawamura, S., Yamamoto, T., Ishida, D., Ogata, T., Nakayama, Y., Tabata, O., and Sugiyama, S., 2002. "Development of passive elements with variable mechanical impedance for wearable robots". In IEEE Interternational Conference on Robotics and Automation, pp. 248–253.
[16] Morita, T., and Sugano, S., 1995. "Design and development of a new robotic joint using a mechanical impedance adjuster". In IEEE International Conference on Robotics and Automation, Vol. 3, pp. 2469–2475.
[17] Hollander, K., Sugar, T., and Herring, D., 2005. "Adjustable robotic tendon using a 'jack spring'tm". In IEEE International Conference on Rehabilitation Robotics.
[18] Shigley, J., 1977. *Mechanical Engineering Design*. McGraw-Hill, New York.
[19] Merz, R., B., P. F., Ramaswami, K., Terk, M., and Weiss, L. E., 1994. "Shape deposition manufacturing". In Proceedings of the Solid Freeform Fabrication Symposium.
[20] Barbero, E., 1999. *Introduction to Composite Materials Design*. Taylor and Francis Inc.
[21] Howell, L. L., and Midha, A., 1996. "Parametric deflection approximations for initially curved, large-deflection beams in compliant mechanisms". In Proceedings of the ASME Design Engineering Technical Conference.
[22] Howell, L. L., 2001. *Compliant Mechanisms*. Wiley, New York.